Eur. Phys. J. D **23**, 15–24 (2003)
DOI: 10.1140/epjd/e2003-00007-y

THE EUROPEAN PHYSICAL JOURNAL D

The Rydberg atom in collinear static and harmonic electric fields

V.N. Ostrovsky[1,a] and E. Horsdal-Pedersen[2,b]

[1] V.A. Fock Institute of Physics, The University of St Petersburg, 198904 St Petersburg, Russia
[2] Institute of Physics and Astronomy, Aarhus University, 8000 Aarhus C, Denmark

Received 2 May 2002 / Received in final form 23 September 2002
Published online 21 January 2003 –

Abstract. In Rydberg atoms subject to static and harmonic collinear electric fields, intrashell transition can be induced by the first order perturbation from a small perpendicular electric or magnetic field, or by effects of the second order in the major fields. Both mechanisms lead to resonances that are suppressed under certain conditions, and high-frequency interference oscillations in case of non-adiabatic field switching. Recent measurements of microwave ionization signals show very rich and fascinating structures similar to the ones predicted for intrashell mixing. We show that the observed ionization structures may be explained by diabatic electric-field ionization and the consistent use of perturbation theory for intrashell mixing. In particular, the dominant oscillation frequency is successfully interpreted in terms of interference between first and second order transition amplitudes. New predictions are provided. The present approach gives a comprehensive picture of intrashell transitions, which may be tested in future experiments designed to observe such transitions directly.

PACS. 32.80.Rm Multiphoton ionization and excitation to highly excited states (*e.g.* Rydberg states) – 42.50.Hz Strong-field excitation of optical transitions in quantum systems; multiphoton processes; dynamic Stark shift

1 Introduction

Recent experiments by Koch *et al.* [1] and Galvez *et al.* [2] focused on the microwave "ionization" of Rydberg states of hydrogen with initial principal quantum numbers n within the range 39–74. The term "ionization" is synonymous with true ionization *or* excitation to higher shells much closer to the ionization limit than the initial one. The experiment did not separate the two channels. The "ionization" took place inside a microwave cavity as a fast, monoenergetic beam of the hydrogenic Rydberg atoms passed through it. A definite n shell was selectively populated by tunable lasers, but the population was spread over the n^2 degenerate substates of the shell. Selective field-ionization indicated that all substates were populated approximately statistically. The "ionization" was driven by an oscillating electric field of amplitude F_ω and frequency ω in the presence of a collinear, static electric field, F_s. The Rydberg atoms were exposed to the fields for a finite time T as they passed through the cavity. The total electric field at maximum, $F_\mathrm{s} + F_\omega$, was normally strong enough to induce diabatic field-ionization of several (but not all) Stark substates of the n shell (see, for instance, Ref. [3]), but the ionization could also proceed through excitation by the microwave field to higher shells and subsequent static-field ionization in a detection region outside the microwave cavity. The "ionization" process thus involves a large number of initial states, the population of which is not known in detail, and possibly several pathways. This is at first sight an extremely complex problem and one could very well expect *a priori* that it would be governed by statistical distributions and thus be quite featureless. This view, however, is contradicted by a wealth of regular structure unveiled experimentally. For varying F_s and fixed values of F_ω and ω this includes regular series of strong resonances with fast superimposed oscillations. Some resonances were suppressed for specific values of the ratio $F_\omega/F_\mathrm{s,r}$, where $F_\mathrm{s,r}$ is the value of F_s at resonance. It is clear that simplifying mechanisms must exist. It is generally accepted that one such mechanism is intrashell transitions among the substates of the initial shell. This can effectively transfer population from states that are stable against ionization to states that ionize readily, as discussed by experimentalists [1,2] and in related theoretical papers by Oks and Uzer [4–6]. Another simplifying mechanism is diabatic field-ionization directly from some of the substates of the shell n, but not from all. If this is indeed the dominant ionization mechanism then it is quite understandable that the "ionization" signal carries the signature of the intrashell mixing.

Some of the theoretical results derived here were found earlier by the use of methods different from the present ones [1,2,4–6]. These previous results include the positions

[a] e-mail: Valentin.Ostrovsky@pobox.spbu.ru
[b] e-mail: horsdal@ifa.au.dk

of the two series of resonances, one set of suppression conditions, and some fast oscillation frequencies. The present more uniform approach has lead to a new set of suppression conditions, two new oscillation frequencies including most importantly the dominant frequency seen experimentally[1], and exact expressions for intrashell transition probabilities in the limit of weak fields. The dominant oscillation frequency, which was not accounted for by previous analysis and tentatively assigned to experimental imperfections, is explained naturally in terms of interference between first and second order amplitudes. Koch *et al.* [1] showed that the Rydberg atoms as they entered the microwave cavity represented a more or less uniform distribution over all Stark substates with principal quantum number n. The present analysis provides evidence for the complementary conclusion that the electronic state of each Rydberg atom was a *coherent* superposition of such Stark substates.

Our objective has been to characterize the intrashell population redistribution mentioned above. It could be considered either as an essential part of the ionization mechanism for strong $F_{\rm s}$ and F_ω as in the cited experimental work, or for weaker fields as an interesting observable process in its own right. Direct experimental data on probabilities for intrashell transitions driven by oscillating fields of smaller frequency and amplitude do not yet exist but such data are very desirable since they would test critically all the present theoretical predictions including transition strengths.

In Section 2 we provide a comprehensive theory of intrashell mixing based on reduction to two effective two-state problems combined with first- and second order perturbation theory. In Section 3 we discuss the results and compare them with previous theoretical conclusions and the available experimental data. In Section 4 we give representative quantitative examples.

2 Theory of intrashell transitions

We consider Rydberg atoms with principal quantum number n interacting temporarily with collinear static and harmonic electric fields of strengths $F_{\rm s}$ and F_ω, respectively, and directed along the z-axis. The total electric field strength $\mathcal{E}_z(t)$ experienced by the Rydberg atoms is thus

$$\mathcal{E}_z(t) = \lambda_{\rm s}(t)\, F_{\rm s} + \lambda_\omega(t)\, F_\omega\, \cos\omega t, \tag{1}$$

where $\lambda_{\rm s}$ and λ_ω are switching functions ($\lambda_{\rm s}(t \to \pm\infty) = \lambda_\omega(t \to \pm\infty) = 0$). In the cited experimental work $\lambda_{\rm s}$ and λ_ω are equal and determined by the passage of fast, monoenergetic Rydberg atoms through a biased microwave cavity. Within first order perturbation theory (*i.e.* for weak fields) the harmonic field-component does not induce any redistribution of population in the manifold of Stark states if it is collinear with the static field. Such a redistribution appears either within higher orders of perturbation theory or due to the presence of orthogonal fields, which could be stray electric fields, a component of the earths magnetic field, or a small misalignment of the fields in (1). These possibilities were discussed previously and some theoretical analysis with important results was provided [1,2,4–6]. However, the analysis was not complete. The present study intends to complement the picture. We use the simplest theoretical tools and describe both effects within the same framework to provide a unified, comprehensive picture.

2.1 Weak perpendicular fields

In this section we assume that a small static electric ($F_\perp$) or magnetic ($B_\perp$) field is present along the x-axis orthogonal to the major fields (1). Even though this field configuration is relatively simple, the dynamics induced by it within the n^2-dimensional Hilbert space of the shell may seem quite complicated. However, it was recently realized [7] that the intrashell dynamics of Rydberg atoms under the action of electric and magnetic fields with an arbitrary time-dependence, both in magnitude and direction, can be exactly reduced to two *effective two-state problems*[2]. These two-state problems are labeled by the index κ ($\kappa = 1$ or 2), and when the z-axis is chosen as the quantization axis they take the form of coupled equations for two amplitudes $\chi_1^{(\kappa)}$ and $\chi_2^{(\kappa)}$ (see for detail Ref. [7]):

$$\begin{aligned} {\rm i}\frac{\partial\chi_1^{(\kappa)}}{\partial t} &= \frac{1}{2}\,\omega_{\kappa z}(t)\,\chi_1^{(\kappa)} + \frac{1}{2}\,[\omega_{\kappa x}(t) - {\rm i}\omega_{\kappa y}(t)]\,\chi_2^{(\kappa)} \\ {\rm i}\frac{\partial\chi_2^{(\kappa)}}{\partial t} &= -\frac{1}{2}\,\omega_{\kappa z}(t)\,\chi_2^{(\kappa)} + \frac{1}{2}\,[\omega_{\kappa x}(t) + {\rm i}\omega_{\kappa y}(t)]\,\chi_1^{(\kappa)}. \end{aligned} \tag{2}$$

Each of the problems is governed by its own time-dependent vector $\boldsymbol{\omega}_1(t)$ or $\boldsymbol{\omega}_2(t)$ defined by

$$\begin{aligned} \boldsymbol{\omega}_1(t) &= \frac{3}{2}\,n\,\boldsymbol{\mathcal{E}}(t) + \frac{1}{2}\,\mathbf{B}(t), \\ \boldsymbol{\omega}_2(t) &= -\frac{3}{2}\,n\,\boldsymbol{\mathcal{E}}(t) + \frac{1}{2}\,\mathbf{B}(t), \end{aligned} \tag{3}$$

where $\boldsymbol{\mathcal{E}}(t)$ is the electric field, $\mathbf{B}(t)$ the magnetic induction, and n the principal quantum number. In cases when only an electric or only a magnetic field is operative, or when the fields are perpendicular, the two effective two-state problems coincide. We are interested in these situations.

The solution of the effective two-state problem provides us with the transition probability p. The emerging two-state problems (2) could, both formally and physically, be cast as the time-evolution of spin-$\frac{1}{2}$ particles subject to time-dependent "magnetic" fields $\boldsymbol{\omega}_1(t)$ or $\boldsymbol{\omega}_2(t)$.

[1] The fast oscillations are not always present in the cited experimental data and the experimentalists have recently cast some doubt on the origin of the oscillations as well as on the interactions previously thought to be responsible for the observed "ionization" (see abstracts of the May 2001 DAMOP meeting).

[2] Below we follow the scheme of the cited paper; a more formal treatment was given by Fursa and Yudin [8] who also discussed earlier attempts of reduction.

In these terms, p is the probability of spin-flip transitions. Avoiding details fully exposed by Kazansky and Ostrovsky [7] (see also the paper by Kazansky *et al.* [9]) we briefly demonstrate the application and power of the effective two-state reduction by a relevant example. Consider the situation when the uppermost Stark state is initially populated. This state has maximum possible value $k = n-1$ of the Stark quantum number $k = n_1 - n_2$ (n_1 and n_2 are conventional parabolic quantum numbers [10]). The probability of transition into a state with arbitrary k, summed over all possible values of the azimuthal quantum number m, is given by the simple formula

$$\mathcal{P}_k = C_{2n-2}^{n-1-k}\, p^{n-1-k}\,(1-p)^{n-1+k}, \tag{4}$$

where

$$C_n^m = \frac{n!}{m!\,(n-m)!} \tag{5}$$

is the binomial coefficient. In particular, the probability of survival in the initial state is

$$\mathcal{P}_{\rm surv} = \mathcal{P}_{n-1} = (1-p)^{2n-2}. \tag{6}$$

Contrary to previous theoretical papers [4–6] we do not use quasi-energy or Floquet formalism[3]. The important features of the experimental observations stem from the fact that a Rydberg atom spends a *finite* time under the action of the fields. This makes the quasi-energy description inconvenient since it does not account in a natural way for non-adiabatic field switching. Below we presume that the field switching functions $\lambda_{\rm s}(t)$ and $\lambda_\omega(t)$ are identical step functions and comment later on a more general case. This means that $\lambda_{\rm s}(t) = \lambda_\omega(t) = 1$ for $-T/2 < t < T/2$ and zero otherwise. Note also that we do not restrict our analysis to resonance situations as in the paper by Oks and Uzer [4], *i.e.* no special relation between the spacing $\omega_{\rm S} = \frac{3}{2}nF_{\rm s}$ of Stark sublevels and the harmonic field frequency ω is presumed.

The weakness of the perpendicular fields allows us to limit the analysis of the effective two-state problem (2) to first order non-stationary perturbation theory. The amplitude of a non-adiabatic transition is evaluated in the standard way as (see, for instance, book by Landau and Lifshits [10])

$$a(F_{\rm s}) = -{\rm i}\,\mathcal{A}\,I, \tag{7}$$

$$I \equiv \int_{-T/2}^{T/2} \exp\left[{\rm i}\,\frac{3}{2}n\left(F_{\rm s}\,t + \frac{1}{\omega}F_\omega\,\sin\omega t\right)\right]{\rm d}t, \tag{8}$$

where

$$\mathcal{A} = \frac{3}{4}nF_\perp \qquad \text{or} \qquad \mathcal{A} = \frac{1}{4}B_\perp \tag{9}$$

for perturbation by an electric or a magnetic field, respectively. We have chosen to treat $F_{\rm s}$ as the independent variable and F_ω, ω, and T as parameters. Formula (4) shows, for the particular case of the uppermost Stark state, that the two-state "spin-flip" probability $p(F_{\rm s}) = |a(F_{\rm s})|^2$ provides all the state-to-state probabilities to the lowest non-vanishing order over the perturbing field. This observation is actually a general one, and not limited to a specific initial state. The lowest order corresponds to a high power of the perturbing field strength, namely to the power $2(n-1-k)$. In particular, the high power to which $1-p$ is raised in formula (6) leads to strong suppression of survival even if p is small. This *amplification effect* is non-linear in p. Indeed, approximating formula (6) by a first-order expansion, $\mathcal{P}_{\rm surv} \approx 1-(2n-2)p$, is unnecessary and strongly restrictive, being valid only for $p \ll 1/(2n-2)$, whereas (6) remains valid under significantly less stringent conditions, $p \ll 1$.

It is convenient to employ a standard expansion of the exponent in terms of Bessel functions $J_m(\beta)$ [11][4]

$$\exp({\rm i}\beta\sin\omega t) = \sum_{m=-\infty}^{m=\infty} J_m(\beta)\,\exp({\rm i}m\omega t). \tag{10}$$

It allows the time integration in (8) to be carried out

$$I = 2\sum_{j'=-\infty}^{j'=\infty} (-1)^{j'}\,J_{j'}(\beta)\,\Delta_{j'}(F_{\rm s},T,\omega), \tag{11}$$

$$\beta \equiv \frac{3n}{2\omega}F_\omega, \tag{12}$$

$$\Delta_{j'}(F_{\rm s},T,\omega) \equiv \frac{\sin\left[(T/2)(3nF_{\rm s}/2 - j'\omega)\right]}{3nF_{\rm s}/2 - j'\omega}. \tag{13}$$

These equations show how $a(F_{\rm s})$ depends on the parameters F_ω, ω, and T. We now discuss these dependences.

"Potentially" (*i.e.* in the limit $\omega T \to \infty$ corresponding to a purely monochromatic field) all functions $\Delta_{j'}(F_{\rm s},T,\omega)$ yield delta-functions due to the universally known relation [10]

$$\lim_{\alpha\to\infty}\frac{1}{\pi}\,\frac{\sin^2\alpha x}{\alpha x^2} = \delta(x).$$

The delta-functions correspond to the resonance condition

$$\frac{3}{2}nF_{\rm s} = j'\omega \tag{14}$$

that can be satisfied only for positive integer values of the index j'. It obviously has the meaning of a j'-photon resonance for transitions between adjacent Stark levels, $k \to k \pm 1$. In case of a purely monochromatic field this condition plays the role of a strict selection rule. In practice, a finite number of harmonic field cycles are seen by a Rydberg atom during the time T that it spends

[3] A quasienergy approach within the formalism of effective two-state problems was discussed by Kazansky and Ostrovsky [7] and Kazansky *et al.* [9].

[4] This mathematical formula is used also in Floquet theory. This leads to some apparent resemblance with that theory. However, as seen from our initial formula (8), we calculate the probability of transition after the operation of a field-pulse and not quasienergies and transition rates as in Floquet theory.

in the field but this number can easily be rather large ($\omega T/2\pi \sim 150$ in the cited experiments), and hence the condition (14) provides a propensity rule. Indeed, the function $\Delta_{j'}(F_{\rm s}, T, \omega)$ is strongly peaked at resonance for $\omega T/2\pi \gg 1$.

We notice that the resonances are suppressed for specific values of the parameter β. For the j'th resonance this happens when the prefactor of the relevant peaked term in (11) equals zero, *i.e.*

$$J_{j'}(3nF_\omega/(2\omega)) = 0. \tag{15}$$

Note, that (15) does not depend on k, so all transitions are suppressed simultaneously.

The resonance peak is superimposed by rapid oscillations due to the phase $3nF_{\rm s}T/4$ in (13). If the static field strength $F_{\rm s}$ is varied at constant T, the oscillations in the transition probability $p(F_{\rm s}) = |a(F_{\rm s})|^2$ have the frequency

$$f_1 = \frac{3}{2}nT, \tag{16}$$

which depends neither on the parameters of the harmonic field nor on the strength of the perturbing orthogonal field.

Even though the frequency f_1 was not the dominant one found experimentally by Koch *et al.* [1], it was indeed seen. The most pronounced frequency was a factor-of-two smaller than f_1. Koch *et al.* (1999) tentatively suggested that T should be replaced by $\frac{1}{2}T_{\rm int}$, where $T_{\rm int}$ is the time actually spent by the atoms in the microwave cavity. The factor $\frac{1}{2}$ should reflect the presence of a microwave-coupling hole in the midplane of the interaction cavity. This hypothesis would bring (16) into agreement with the dominant frequency observed experimentally, and it was indeed used by Oks and Uzer [6] who were the first to derive expression (16). However, the hypothesis was never substantiated and Galvez *et al.* [2] later concluded that in fact the perturbation of the microwave field is small. An alternative explanation of the dominant frequency is suggested in Section 2.3 of this paper.

While the oscillation frequency is given by the simple formula (16), the amplitude is generally a complicated function of all the parameters. It is given by the interplay of the Bessel functions in (11) and the denominators in the expressions for $\Delta_{j'}(F_{\rm s}, T, \omega)$ (13). In order to illustrate the behaviour we consider $\mathcal{P}_{\rm surv}$ near the $j' = 1$ resonance for small values of β, *i.e.* for $3nF_{\rm s}/2 \simeq \omega$ and $3nF_\omega/2 \ll \omega$. The probability of survival $\mathcal{P}_{\rm surv}$ is then estimated by taking the square of the resonance term and applying it in (6)

$$\mathcal{P}_{\rm surv} = \left[1 - \left(\mathcal{A}\frac{3n}{2\omega}F_\omega\right)^2 \frac{\sin^2\left[(T/2)(3nF_{\rm s}/2-\omega)\right]}{(3nF_{\rm s}/2-\omega)^2}\right]^{2n-2}. \tag{17}$$

The high power, $2n-2$, strongly amplifies the oscillations, so instead of having a narrow resonance dip with small separated dips on each side, which would be the result if $2n-2$ were small, one expects to see a broadened resonance dip with overlapping damped oscillations.

The state-to-state transition probabilities contain integer powers of $p(F_{\rm s})$ (see formula (4)). Therefore, harmonics f_q of the frequency f_1 appears in a Fourier spectrum of $\mathcal{P}_{\rm surv}(F_{\rm s})$ ($f_q = qf_1$ with integer q). Furthermore, $\mathcal{P}_{\rm surv}$ is not strictly a periodic function of $F_{\rm s}$ because of the $F_{\rm s}$-dependence of the denominator in the expression for $\Delta_{j'}(F_{\rm s}, T, \omega)$ (13). The Fourier spectrum could therefore also show "smaller peaks at values of f that are not integral multiples of f_1" [1].

2.2 Second-order effects

The intrashell second-order effects in the electric field were reduced by Solov'ev [12] to the convenient form of an equivalent operator

$$\hat{W} = -\mathcal{E}^2\,\frac{n^4}{16}\left(5n^2 + 31 + 24L^2 - 21L_z^2 + 9A_z^2\right), \tag{18}$$

where $\mathbf{L}$ and $\mathbf{A}$ are the electron angular momentum and Runge-Lenz operators, respectively (the electric field is directed along z-axis). In the basis of Stark states this operator has diagonal matrix elements

$$\langle n\,k\,m\,|\hat{W}|n\,k\,m\rangle = -\mathcal{E}^2\frac{n^4}{16}(17n^2 + 19 - 9m^2 - 3k^2) \tag{19}$$

that give the well-known quadratic Stark shifts of hydrogen energy levels, but most importantly, the non-diagonal matrix elements

$$\langle n\,k+2\,m\,|\,\hat{W}\,|n\,k\,m\rangle = \langle n\,k\,m\,|\,\hat{W}\,|n\,k+2\,m\rangle = \mathcal{E}^2\,\mathcal{C}_{k\,m},$$
$$\mathcal{C}_{k\,m} = \frac{3}{8}n^4\sqrt{[(n-k-1)^2 - m^2][(n+k+1)^2 - m^2]} \tag{20}$$

couple Stark states of quantum numbers k and $k \pm 2$. All other non-diagonal matrix elements vanish[5].

The second-order effects resulting from (virtual) intershell transitions cannot be treated within the reduction scheme of the previous section. We employ instead conventional first-order non-stationary perturbation theory (Landau and Lifshits [10]). The amplitudes of the transitions $k \to k+2$ induced by the operator (18) are evaluated in terms of the standard integral (8) *but with doubled arguments*:

$$\begin{aligned} b(F_{\rm s})_{k\to k+2} &= -{\rm i}\,\mathcal{C}_{k\,m}\int_{-T/2}^{T/2}{\rm d}t\;(F_{\rm s} + F_\omega\,\cos\omega t)^2 \\ &\quad\times\exp\left[{\rm i}\,3n\left(F_{\rm s}\,t + \frac{1}{\omega}F_\omega\,\sin\omega t\right)\right] \\ &= {\rm i}\,\mathcal{C}_{k\,m}\,F_\omega\left(\frac{\omega}{3n}\right)^2\frac{\rm d}{{\rm d}F_\omega}\int_{-T/2}^{T/2}{\rm d}t \\ &\quad\times\exp\left[{\rm i}\,3n\left(F_{\rm s}\,t + \frac{1}{\omega}F_\omega\,\sin\omega t\right)\right] + \mathcal{Q} \\ &= 2{\rm i}\,\mathcal{C}_{k\,m}\left(\frac{\omega}{3n}\right)^2\sum_{j=-\infty}^{j=\infty}(-1)^j\,2\beta\,J_j'(2\beta) \\ &\quad\times\Delta_j(2F_{\rm s}, T, \omega) + \mathcal{Q}. \end{aligned} \tag{21}$$

[5] The same result was rederived recently by Oks and Uzer [4] within their "robust perturbation theory" [13].

The term

$$\mathcal{Q} = -\mathrm{i}\,\frac{2}{3n}\,\mathcal{C}_{k\,m}\left[F_\mathrm{s} + F_\omega\,\cos\left(\frac{1}{2}\,\omega T\right)\right] \times \sin\left[\frac{3}{2}nF_\mathrm{s}T + \frac{3}{\omega}nF_\omega\,\sin\left(\frac{1}{2}\,\omega T\right)\right] \qquad (22)$$

comes from integration by parts and is not of particular interest here since it is not of resonance nature. The origin of the argument doubling is simple. Standard nonstationary perturbation theory implies integration over time t with the characteristic exponent $\mathrm{i}\int^t \Delta E(t')\,\mathrm{d}t'$ in the integrand, as in formulae (8) or (21). The perpendicular field induces transitions between adjacent Stark states, $\Delta k = \pm 1$, whereas for the second order effect the transition energy ΔE is twice as large, since $\Delta k = \pm 2$. Our result (21) could be compared with formula (56) obtained by Oks and Uzer [4], which in our notation equals $\mathcal{C}_{k\,m}\,\omega^2\,(-1)^j\,2\beta J_j'(2\beta)$. It does not include the interference factor Δ_j and is thus valid only at exact resonance.

The structure of formula (21) is qualitatively similar to that of expression (11), although there are important quantitative differences. In particular, according to formula (21) instead of the resonance condition (14) we now have

$$3nF_\mathrm{s} = j\omega. \qquad (23)$$

The origin of the difference is clear: the second order effects only induce transitions with a change of the Stark quantum number k by ± 2, whereas for perpendicular fields transitions between adjacent Stark levels, $k \to k \pm 1$, is possible. The resonance transitions are suppressed if

$$J_j'(3nF_\omega/\omega) = 0. \qquad (24)$$

This condition coincides with the one suggested by Galves *et al.* [2] and Oks and Uzer [4]. It is in good agreement with the experimental data, as discussed by these authors. Note that *all* the transitions $k \to k \pm 2$ are suppressed simultaneously, independent of k. It is evident from a comparison between (11) and (21) that the second-order transitions lead to fast oscillations at the frequency $f_2 = 2f_1$. The characteristics of these oscillations are similar to the ones discussed in the previous section.

2.3 Amplitude interference effects

In this section we consider the possibility that each Rydberg atom is initially described by a coherent superposition of Stark states $|n,k,m\rangle$ of energy E_k, $\psi(t) = \sum_{k,m} A_{k,m}|n,k,m\rangle \exp(-\mathrm{i}E_k t)$. The amplitude for transition to a final Stark state $|n,k,m\rangle$ induced by the field-pulse has contributions from the states $|n,k\pm1,m\rangle$ due to weak perpendicular fields and from $|n,k\pm2,m\rangle$ due to second order effects. To expose the essential effects of this coherence we consider the total amplitude for small values of β and near the single-photon resonances. According to formulae (11) and (21) it has the form

$$a_k = D_1\beta\Delta_1(F_\mathrm{s},T,\omega) + D_2\beta\Delta_1(2F_\mathrm{s},T,\omega) = \left[D_1\frac{\sin\left[(T/2)(3nF_\mathrm{s}/2-\omega)\right]}{3nF_\mathrm{s}/2-\omega} + D_2\frac{\sin\left[(T/2)(3nF_\mathrm{s}-\omega)\right]}{3nF_\mathrm{s}-\omega}\right]\beta, \qquad (25)$$

where the constants D_1 and D_2 depend on the strengths of the two transition mechanisms and on the population of the contributing initial Stark states. The interference term in $|a_k|^2$

$$p_\mathrm{int} = 2\beta^2\,\mathrm{Re}(D_1D_2)\,\frac{\sin\left[(T/2)(3nF_\mathrm{s}/2-\omega)\right]}{3nF_\mathrm{s}/2-\omega} \times\frac{\sin\left[(T/2)(3nF_\mathrm{s}-\omega)\right]}{3nF_\mathrm{s}-\omega} = \beta^2\,\mathrm{Re}(D_1D_2) \times\frac{\cos\left[(3/4)nTF_\mathrm{s}\right]-\cos\left[(9/4)nTF_\mathrm{s}-\omega T\right]}{(3nF_\mathrm{s}/2-\omega)(3nF_\mathrm{s}-\omega)} \qquad (26)$$

shows oscillations of comparable amplitude at the frequencies

$$f_\mathrm{int} = \frac{1}{2}f_1 = \frac{3}{4}nT \qquad \text{and} \qquad 3f_\mathrm{int}. \qquad (27)$$

The dominant frequency observed experimentally agrees exactly with f_int.

The dependence of the transition probability on the perturbation parameter $\mathcal{A}$, which is proportional to the strength of the perpendicular field (Sect. 2.1), is as follows. A perpendicular field alone induces transitions with probability $p \sim D_1^2 \sim \mathcal{A}^2$, whereas the interference term behaves as $p_\mathrm{int} \sim 2\mathrm{Re}(D_1D_2) \sim \mathcal{A}$. If the perturbation $\mathcal{A}$ is small (for instance, being induced by weak stray electric fields) then p may be vanishingly small, but the interference term p_int prevails provided second order effects are significant. In other words, interference effectively enhances the influence of stray fields in the regime where transitions are induced mainly by the second-order effects.

3 Discussion

3.1 Resonance position

Considering the two resonance conditions obtained, we notice that all resonances satisfying condition (23) (second-order effects) also satisfy condition (14) (perpendicular-field effects), but the reverse statement is not true. Every perpendicular-field resonance is masked by a second-order resonance ($2j' = j$), but the second-order resonances of odd j are pure and since they are observed in the experiments, the second-order mechanism is definitely operative. It is more difficult to judge whether perpendicular-field resonances are present, since they are always veiled. It can be noted, however, that the experimental data displayed in Figure 1 of the paper by Galves *et al.* [2] exhibit

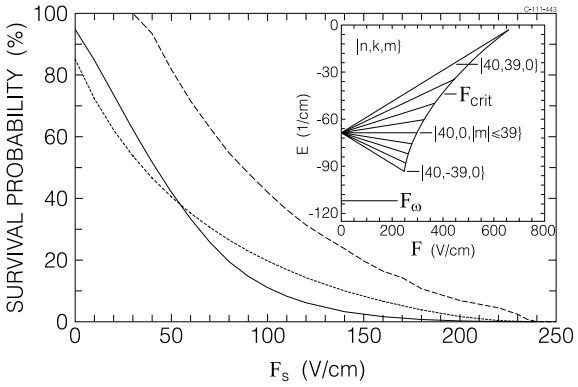

Fig. 1. Survival probability $P_{\rm pass}$ against diabatic electric field ionization for three ensembles of Rydberg atoms with $n = 40$ at $F_\omega = 220$ V/cm, $\omega = 2\pi \times 8.1$ GHz, and $T = 16.9$ ns. Full curve, uniform distribution on all n_1, n_2, and m. Dotted curve, uniform distribution on all n_1 and n_2, but $|m| \leq 3$. Broken curve, uniform distribution on $0 \leq k = n_1 - n_2 \leq 39$ and $m = 0$. Compare with Figure 1 in Galves *et al.* [2]. Inset shows a few states of the $n = 40$ Stark manifold and critical fields $F_{\rm crit}$ satisfying $\Gamma(F_{\rm crit}) = 10^9\,{\rm s}^{-1}$.

a significantly more pronounced and broadened resonance for $j = 2$ than for $j = 1$. This could be tentatively related to the fact that in the former case both mechanisms work jointly whereas in the latter only the second-order mechanism is operative. The appearance of the oscillation frequency $f_{\rm int}$ is further evidence that perpendicular-field effects are indeed operative, since otherwise the related interference effects vanish.

3.2 Resonance suppression

Using (23) one can rewrite the suppression condition (24) of resonances induced by second-order effects to the form employed by Galves *et al.* [2]:

$$J'_j(jR) = 0, \qquad R = F_\omega/F_{\rm s,r}. \tag{28}$$

Condition (15) for the suppression of resonances induced by perpendicular fields can be cast in a similar form

$$J_{j'}(j'R) = 0. \tag{29}$$

The suppression condition (28) pertaining to second-order effects was tested by Galves *et al.* [2] who indeed found suppression at the first non-trivial zero of $J'_j(jR)$ for $j = 2$, 3, and 4, and at the second non-trivial zero of $J'_1(R)$. However, the condition (29) from perpendicular fields has not yet been examined experimentally. For $j' = 1$ and 2, the first non-trivial zeroes of $J_{j'}(j'R)$ are at $R = 3.832$ and 2.568, respectively. The suppression at these R-values may not be complete because each perpendicular-fields resonance is masked by a second-order resonance as discussed in Section 3.1, and the two resonance mechanisms lead to suppression at different values of R. However, this is not a disadvantage since it allows for separate tests of the two suppression conditions. For instance, experimentalists [2] saw suppression of the resonance at $F_{\rm s} = 2\omega/3n$ near $R = 1.527$ ($j = 2$), but it should be suppressed also at $R = 3.832$ ($j' = 1$). Similarly, the resonance at $F_{\rm s} = 4\omega/3n$ should be suppressed not only at $R = 1.326$ ($j = 4$) but also at $R = 2.568$ ($j' = 2$). Experimental data to test (29) at the mentioned R-values of 3.832 and 2.568 are very desirable.

3.3 High-frequency oscillations under $F_{\rm s}$ variation

The high-frequency oscillations derived and discussed in Section 2 are crucially related to the non-adiabatic switching of the electric fields. When the fields are switched on non-adiabatically they are likely to populate coherently a range of Stark substates of different energies, and the resulting interference or beat pattern is "registered" as the field is switched off. The sudden switching presumed in the present calculations emphasizes the effect, but it persist for any form of switching functions $\lambda_{\rm s}(t)$ and $\lambda_\omega(t)$, provided they are sufficiently steep. For smoother switching these oscillations tend to disappear.

Oscillations at the frequency $2f_1$ should be seen near the lowest-lying resonance caused by the second-order effects only, and oscillations at the two frequencies f_1 and $2f_1$ should be seen near the next resonance caused by second-order effects as well as perpendicular fields. The frequencies f_1 and $2f_1$ were both seen in the experiments but they were not correlated with the resonance structure and neither of them were dominant. A Fourier analysis of the data in selected segments of $F_{\rm s}$ would test the predicted correlation. Note that according to formula (26) the frequencies $f_{\rm int}$ and $3f_{\rm int}$ (27) are present near both types of resonance.

The amplitude interference terms showing oscillations at the frequencies $f_{\rm int}$ and $3f_{\rm int}$ are present only when the initial Rydberg atoms are prepared in a coherent superposition of Stark substates (see Sect. 2.3). It seems that coherence conditions were met in the experiments. Full experimental detail was given by Koch and van Leeuwen [14] and Koch *et al.* [1]. A monoenergetic beam of accelerated protons (14 keV) was partially neutralized in a gas cell, and when the resulting hydrogen atoms entered a region of high electric fields, some of them were excited to an extremal Stark state by laser excitation. During flight from the high-field domain to the microwave cavity the Rydberg atoms traversed a region, which was intended to be field-free, but where they actually were influenced by uncontrolled stray electric fields. This led to an ensemble of atoms which in selective field ionization was consistent with a uniform distribution of population over all substates of the shell. The Rydberg atoms used in the experiments were tightly collimated and quite monoenergetic. All atoms thus experienced the same field variation as they passed the region of stray electric fields, so an ensemble of atoms in identical coherent superpositions of Stark states, could be formed already in this region, and not just a statistical distribution. The presumption is supported by the following estimate. A realistic stray field of

less than 500 mV/cm leads to a Stark period longer than about 20 ns for a typical n value. The interaction time was about 50 ns corresponding to a flight distance of 10 cm. The very small fluctuations of this time ($\leq$1% of 50 ns) are small compared to the Stark period ($\geq$20 ns). It is thus likely that phases are well-defined and a coherent superposition is formed.

Coherent superpositions could also be formed at the entrance to the microwave cavity. The electrically isolated endcaps of the cavity were symmetrically biased ($\pm V/2$ volts) to form the static electric field, $F_{\rm s}$, inside the cavity. As the Rydberg atoms approached the cavity from ground potential and flew into it, they therefore felt a longitudinal field which went to zero and changed direction somewhere inside the long, cylindrical entrance hole of the first endcap (diameter 2.0 mm and length 6.4 mm). The Rydberg atoms passed the endcap in less than 4 ns, and during this time the atoms saw an electric field which varied by typically 100 V/cm. Even when the non-linear variation of the field within the hole is taken into account, the rate-of-change of the field as seen by the Rydberg atoms was large near the position where the field was close to zero and where the Rydberg atoms were the least stabilized by the field. A well-defined instant of time for state mixing thus exists which would also lead to a coherent superposition.

The expression (26) for the amplitude interference term leads to the frequencies $f_{\rm int} = \frac{1}{2} f_1$ and $3f_{\rm int}$ of which the first agrees exactly with the dominant frequency seen experimentally [1]. Oscillations at the frequency, $f_{\rm int}$, permeates the full range of $F_{\rm s}$-values in good agreement with the double-resonance structure of (26). The oscillations at the higher frequency, $3f_{\rm int}$, should be exactly as intense as the ones at $f_{\rm int}$. This does not agree with the experimental results, which show a much reduced strength. However, this is most likely due to a broadening mechanism that masks the higher frequencies. We conclude that the Rydberg atoms are in coherent superpositions of Stark states as they enter the microwave cavity, that both mechanisms of intrashell transitions are operative, and that they interfere as discussed in Section 2.3.

4 Representative quantitative examples

4.1 Diabatic field ionization

A quasistatic electric field that rises slowly does not mix hydrogenic Stark states belonging to different shells, and the electric field dependent energy levels cross freely or diabatically (for a detailed discussion see, for instance, book by Gallagher [15]). The rising field will eventually lead to the ionization of the atom. For a given Stark state this takes place at a quite well-defined value of the field strength when the overlap between the bound Stark state and the continuum of free Stark states has become sufficiently large. The electron then tunnels through the potential barrier that separates the bound and the continuum states. The electric-field dependent rate coefficient for the tunneling, Γ, was analyzed, among others, by Damburg and Kolosov [3] who gave a convenient closed analytical expression that covers all Stark states, $\Gamma = \Gamma_{n,n_1,n_2,m}(F)$ where n, n_1, n_2, and m are parabolic quantum numbers and F the field strength. Stark states with electric dipole moment parallel to the field are depressed in energy and they ionize at a smaller field-strength than states of antiparallel dipole moment that are raised in energy. Critical fields corresponding to $\Gamma = 10^9$ s^{-1} for $n = 40$ are shown in the inset of Figure 1. It is clear that the maximum fields normally present in the microwave cavity used in the experiments are sufficiently strong to ionize a considerable part of the downshifted Stark states (220–470 V/cm, [2]). The experiments determined the probability for an atom to pass the cavity without being ionized, $P_{\rm pass} = \exp\left[-\int_{-T/2}^{T/2} \Gamma(F(t))\mathrm{d}t\right]$. In order to be able to calculate this quantitatively, we utilized the fact that ionization takes place only within short intervals around the time t_m when $F(t)$ is near its maximum value F_m. $\Gamma(F(t))$ is very strongly peaked in these intervals with a maximum value of Γ_m. The following approximations are therefore justified. $\Gamma(F)$ is expanded to first order around F_m, and $(F - F_m)$ is expanded to second order around $t = t_m$. This leads to $\Gamma(t) = \Gamma_m - \frac{1}{2} F_\omega [\mathrm{d}\Gamma(F_m)/\mathrm{d}F]\omega^2 (t - t_m)^2$. The integral of Γ was taken over the time intervals for which $\Gamma(t) \geq \Gamma_m/2$. It can be calculated analytically, but we do not give the expression here. It takes the values $I = N I_{n,n_1,n_2,m}(F_{\rm s}, F_\omega, \omega)$, where N is the number of cycles seen by the atom. With this we finally get $P_{\rm pass} = \exp(-I)$. Figure 1 shows $P_{\rm pass}(F_{\rm s})$ for $n = 40$, $F_\omega = 220$ V/cm, $\omega = \Omega_0 \equiv 2\pi \times 8.1$ GHz, and for a few substate distributions. The distribution actually used in the experiments is unknown but Galves *et al.* [2] mention a uniform distribution on all substates as a likely possibility. We show $P_{\rm pass}$ for this distribution and for two distributions over states of low angular momentum. The calculations should be compared to the experimental data shown in Figure 1 of Galves *et al.* [2]. Although the agreement is not perfect, it is indeed fairly good, so we conclude that the ionization mechanism is diabatic field ionization directly from the initial shell n.

4.2 Perpendicular field effects

We discuss only the effect of a perpendicular electric field since perpendicular electric and magnetic fields are treated on the same footing (9). The choice of field parameters is guided by the experiments [1,2]. In particular, we choose the microwave frequency $\omega = \Omega_0$ and consider Rydberg atoms with principal quantum number $n = n_0 \equiv 45$. Figure 2 shows high-frequency oscillations in the survival probability (6) with $p = |a(F_{\rm s})|^2$ given by (7) and (11). This could be compared with the lower curve in Figure 9 of [1]. The time T is taken as the *full* time spent by an atom in the microwave cavity, *i.e.* $T = T_{\rm int} \equiv L/v = 15.9$ ns where $L = 2.758$ cm is the cavity length and $v = 1.73 \times 10^6$ m/s is the velocity of the H atoms (15.8 keV). Figure 2 shows rapid oscillations of frequency f_1 (16) in striking disagreement with

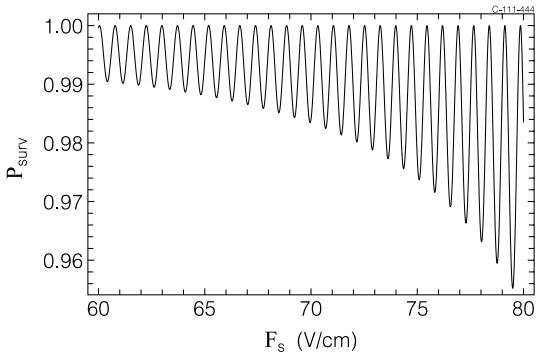

Fig. 2. High-frequency oscillations of the survival probability in the outermost Stark state of a H($n = 45$) atom. The oscillations are induced by a small field component ($F_\perp = 0.6$ V/cm) perpendicular to collinear static F_s and microwave F_ω fields. $F_\omega = 152$ V/cm, $\omega = 2\pi \times 8.1$ GHz, and $T = 15.9$ ns.

the dominant experimental frequency, which is two times lower. Oks and Uzer [4] replace T by $\frac{1}{2}T_\mathrm{int}$ to eliminate the disagreement but the justification for doing so is weak. We demonstrated already in Section 2.3 under simplifying assumptions that an interference term oscillates at $f_1/2$ in agreement with the experimental data. In Section 4.4 we show numerically without simplifying assumptions how the lower frequency emerges. It should be noted also that the depth of modulations in Figure 2 increases with F_s. This again is in disagreement with the experimental results, but as we shall see, the interference term leads to an almost constant modulation depth in good agreement with experiment.

In our calculations we have chosen a perpendicular field component of $F_\perp = 0.6$ V/cm. This field could come from a small misalignment of the static and microwave fields ($F_\perp/F_\mathrm{s} \approx 0.004$ rad) or from stray electric charges. A magnetic field of $B_\perp \approx 38$ Gauss would have the same effect ($n = 45$), but this field is unrealistically high, so the perpendicular field is most likely electric. The chosen field, $F_\perp$, gives depths of modulation between 1% and 4% (Fig. 2), which are representative for some experimental results (see Fig. 6 in the paper by Koch *et al.* [1]). In the regime considered here the modulation depth $1-\mathcal{P}_\mathrm{surv} \sim p$ is proportional to $F_\perp^2$.

Figure 3 shows the $j' = 1$ resonance of the perpendicular-field effect and its suppression at $R = 3.832$ (Eqs. (6, 7, 11)). In order to avoid electric fields near suppression far beyond the ionization limit, we take $\omega = \frac{1}{4}\Omega_0$ in this example. The resonance then lies at $F_\mathrm{s} = 23.45$ V/cm and it is suppressed at $F_\omega = 89.84$ V/cm. Note that this type of resonance suppression has not been tested experimentally. The fast oscillations seen in Figure 3 are given predominantly by the $j' = 1$ term in (11), but they are modulated near the resonance by other terms of low j'.

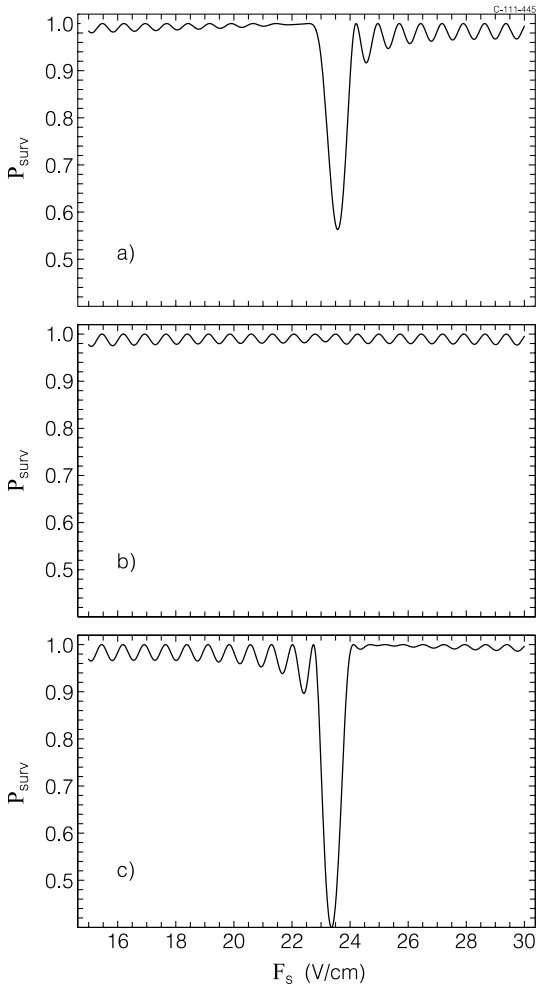

Fig. 3. The $j' = 1$ resonance in H($n = 45$) induced by a perpendicular field ($F_\perp = 0.6$ V/cm) is shown for three values of F_ω. $T = 16.9$ ns and $\omega = 2\pi \times 2$ GHz. The resonance is suppressed at $F_\omega = 89.84$ V/cm (b), but strong just below (88 V/cm) (a) and above (92 V/cm) (c).

4.3 Second-order effects

The $j = 2$ two-photon resonance and its suppression at $R = 1.527$ is illustrated in Figure 4 for the standard parameters ($\omega = \Omega_0$, $n = n_0$). We first concentrate on the position of the resonance. According to formula (23) one should expect to see the resonance at 93.8 V/cm, but it was observed at about 88V/cm (Fig. 2 in Galves *et al.* [2]). The reason for this quite significant shift of 6% was not discussed. However, within the present theory we can comment on it. The k-dependent part of the Stark shift in the first and second orders of perturbation theory reads (*cf.* Eq. (19)):

$$\delta E_k = \frac{3}{2}nk\mathcal{E} + \frac{3}{16}n^4k^2\mathcal{E}^2. \qquad (30)$$

From this formula we see that the spacing between adjacent Stark sublevels is independent of k to first order, but it becomes k-dependent when second order terms are included. The $k = 0$ level in the middle of the Stark spectrum is unshifted, but in the lower part of the spectrum ($k < 0$) the levels are increasingly compressed whereas the spacing increases in the upper part ($k > 0$). The latter is the more essential part for ionization enhancement,

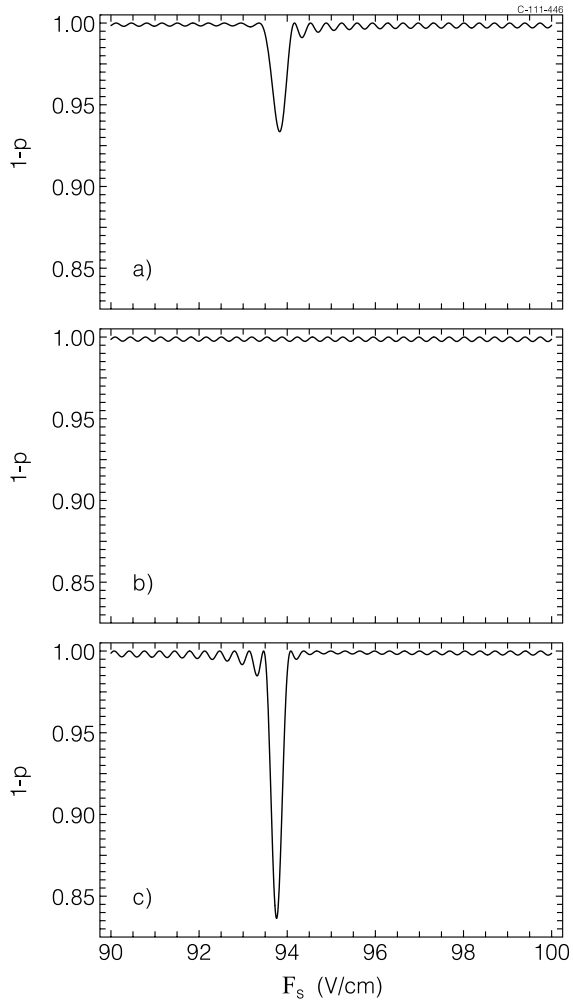

Fig. 4. The $j = 2$ resonance in H($n = 45$, $k = 0$) induced by second-order effects is shown for three values of F_ω. $T = 16.9$ ns and $\omega = 2\pi \times 8.1$ GHz. The resonance is suppressed at $F_\omega = 143.2$ V/cm (b), but strong just below (139 V/cm) (a) and above (148 V/cm) (c).

because states belonging to this part generally do not ionize (see inset of Fig. 1). Enhancement is due to transfer of population from states in the upper part of the spectrum that do not ionize to states in the lower part that ionize immediately. Since the spacing is increased in the upper part of the spectrum, a resonance with a fixed two-photon energy, 2ω, occurs at a smaller value of F_s, in qualitative agreement with the shift seen experimentally. The shift depends slightly on F_ω (Fig. 2 in Galves *et al.* [2]). We are not in a position to comment on this dependence at present.

Bearing in mind that the shift discussed above is not included in our simple formulae, we can still compare our results shown in Figure 4 with the experimental data (Fig. 2 in Galves *et al.* [2]). To comply with the experimental parameters the velocity v now corresponds to 14 keV/amu, so $T = T_\mathrm{int} = 16.9$ ns. Theory and experiment agree that resonance suppression occurs at $R = 1.527$. When comparing survival probabilities one should note that we show in Figure 4 the probability $1-p$ with $p = |b(F_\mathrm{s})_{k\to k+2}|^2$ for $k = 0$, *i.e.* a substate lying in the center of the Stark manifold. The results represent the survival probability for only this substate, so even though we take it to be representative, the comparison with the experimental data can only be qualitative. Quite naturally, since the calculation takes into account depopulation of only one Stark state it leads to much smaller resonance dips than seen experimentally ($\simeq 1\%$ *vs.* $\simeq 50\%$). The theoretical resonance is substantially deeper above resonance suppression than below. This trend is not seen in the experimental data, perhaps because of saturation effects. The frequency of the fast oscillations seen in Figure 4 is twice the frequency seen in the previous figures.

4.4 Combined picture: Interference effects

We now consider the interference of the two intrashell transition mechanisms and assume complete coherence as in Section 2.3. We use the standard parameters $\omega = \Omega_0$ and $n = n_0$, and $T_\mathrm{int} = 16.9$ ns, $F_\omega = 152$ V/cm, and $F_\perp = 0.6$ V/cm. Figures 5a, 5b, and 5c show $1-p$ for $p = |a(F_\mathrm{s})|^2$, $p = |b(F_\mathrm{s})_{0\to 2}|^2$, and $p = |a(F_\mathrm{s}) + b(F_\mathrm{s})_{0\to 2}|^2$, respectively. Corresponding Fourier spectra are shown in Figures 5d, 5e, and 5f. The first (Fig. 5d) shows that the perpendicular field alone produces oscillations with a single frequency $f_1 = 3nT/2 = 9.12$ (V/cm)$^{-1}$, the second (Fig. 5e) confirms that the second-order effects alone generate oscillations with doubled frequency $2f_1 = 18.24$ (V/cm)$^{-1}$, and the third (Fig. 5f) demonstrates that interference implies two new frequencies, $\frac{1}{2}f_1 = 4.56$ (V/cm)$^{-1}$ and $\frac{3}{2}f_1 = 13.68$ (V/cm)$^{-1}$, in agreement with the analysis in Section 2.3. With the realistic parameters chosen for the present example, the strength of the Fourier component $2f_1$ dominates whereas f_1 is rather small. The two interference components have equal strengths which lie in between the two previous ones. This is in full agreement with our discussion in Section 2.3, interference effectively enhances the influence by stray fields in the regime where transitions are induced mainly by the second-order effects. The experiments do not give equal amplitudes of the interference terms, as discussed in the end of Section 3.3. The periods of the slow and fast interference components are $2\pi/(\frac{1}{2}f_1) = 1.38$ V/cm and 0.46 V/cm, respectively. The strengths of stray electric fields could be comparable to the short period and thus lead to some smearing of the fast oscillations. These would accordingly appear to be weaker than the slow oscillations as observed.

5 Conclusion

Recent experiments on the ionization of Rydberg atoms of H exposed to collinear static and microwave fields were analyzed with special emphasis on intrashell transitions. This has led to a comprehensive theory of intrashell dynamics of hydrogenic Rydberg atoms exposed simultaneously to static and harmonic external fields. Two intrashell

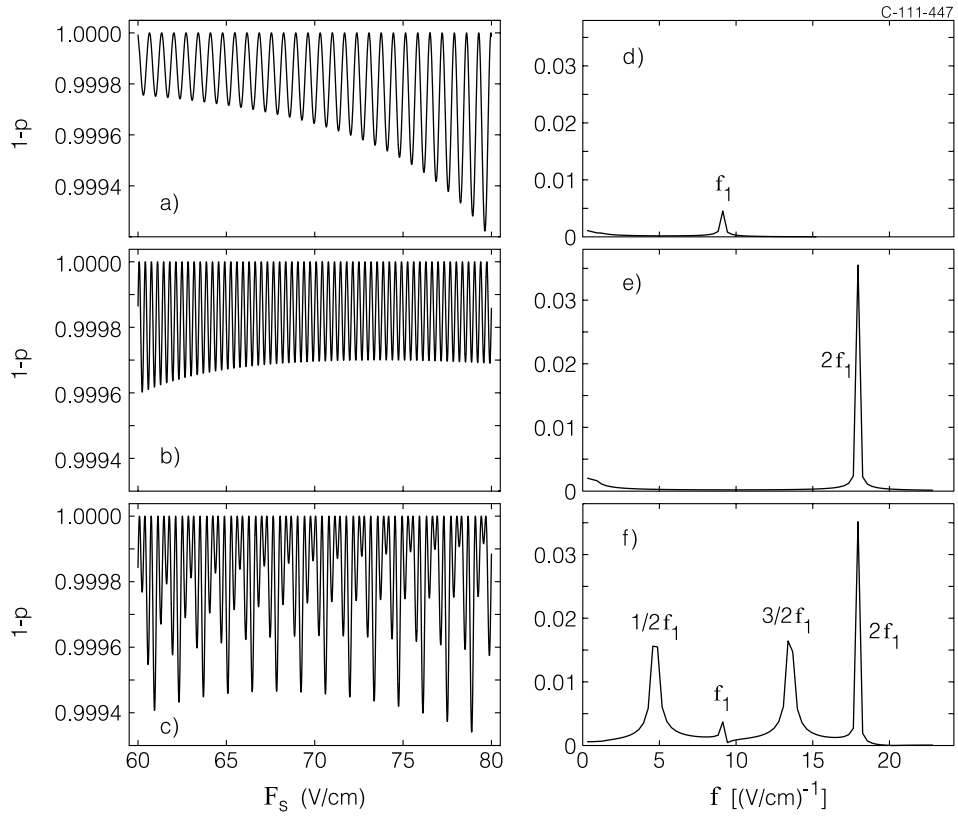

Fig. 5. High-frequency oscillations of $1-p$ for H atom in a microwave field of $\omega = 2\pi \times 8.1$ GHz. Other parameters as in Figures 3 and 4; (a) only perpendicular field effects; (b) second-order effects; (c) both effects under the assumption of complete coherence. Fourier spectra of (a), (b), and (c) are shown in (d), (e), and (f), respectively. The frequencies $f_1 = 3nT/2 = 9.12$ $(\mathrm{V/cm})^{-1}$ and $2f_1$ are seen in (d) and (e), respectively, and (f) shows four frequencies, f_1 and $2f_1$ as well as interference frequencies $\frac{1}{2}f_1$ and $\frac{3}{2}f_1$. Note that the period corresponding to f_1 is $2\pi/f_1 = 0.689$ V/cm.

transition mechanisms were treated and it was shown how they interfere when the initial Rydberg state is a coherent superpositions of Stark substates. Some results obtained in this work were published previously by other authors. Nevertheless, we think that the present treatment is valuable because it offers new predictions on intrashell transitions, it is simple, and it is comprehensive. The comparison with the available experimental data on hydrogen is facilitated by the pure Coulomb potential of the problem, but it is complicated by an unknown initial distribution of population on the Stark substates of the selected shell n and by a somewhat uncertain basic interpretation of the experimental data. It is also (but to a smaller extent) made difficult by the experimental summation over totally different ionization channels that are not separated. The present theory provides specific predictions which can be tested directly in future experiments focused on the intrashell dynamics instead of multistage ionization process.

V.N.O. is thankful for hospitality to the staff of the Institute of Physics and Astronomy, Aarhus University where this work was carried out.

References

1. P.M. Koch, E.J. Galvez, S.A. Zelazny, Physica D **131**, 90 (1999)
2. E.J. Galvez, P.M. Koch, D. Richards, S.A. Zelazny, Phys. Rev. A **61**, 060101 (2000)
3. R.J. Damburg, V.V. Kolosov, J. Phys. B **12**, 2637 (1979)
4. E. Oks, T. Uzer, J. Phys. B **33**, 1985 (2000)
5. E. Oks, T. Uzer, J. Phys. B **33**, 2207 (2000)
6. E. Oks, T. Uzer, J. Phys. B **33**, 5357 (2000)
7. A.K. Kazansky, V.N. Ostrovsky, J. Phys. B **29**, L855 (1996)
8. D.V. Fursa, G.L. Yudin, Phys. Rev. A **44**, 7414 (1991)
9. A.K. Kazansky, H. Nakamura, V.N. Ostrovsky, Laser Phys. **7**, 773 (1997)
10. L.D. Landau, E.M. Lifshitz, *Quantum Mechanics* (Pergamon, Oxford, 1965)
11. I.S. Gradshteyn, I.M. Ryzhik, *Table of Integrals, Series and Products* (Academic, New York, 1965)
12. E.A. Solov'ev, Zh. Éksp. Teor. Fiz. **85**, 109 (1983) [Sov. Phys. - JETP **58**, 63 (1983)]
13. E. Oks, T. Uzer, Europhys. Lett. **49**, 554 (2000)
14. P.M. Koch, K.A.H. van Leeuwen, Phys. Rep. **255**, 289 (1995)
15. T. Gallagher, *Rydberg Atoms* (Oxford University Press, 1994)